On the efficacy of coherence-based assessment of functional coupling between pools of motor units

Leon Kutoš[1], Miloš Kalc[2], Matej Kramberger[1], Filip Urh[1], Aleš Holobar[1]

[1] *Faculty of Electrical Engineering and Computer Science, University of Maribor, Maribor, Slovenia*
[2] *Science and Research Centre Koper, Koper, Slovenia*
E-pošta: leon.kutos@um.si, ales.holobar@um.si

On the efficacy of coherence-based assessment of functional coupling between pools of motor units

Abstract. *We studied the impact of the extension of the convolutive data model of high-density electromyograms (hdEMG) on the accuracy of coherence estimation between the motor unit (MU) activity indices (AI) calculated from different heads of biceps brachii (BB) (in simulated conditions) and gastrocnemius lateralis (GL) and medialis (GM) muscle in 5 young, healthy subjects. AI was calculated for each muscle head (simulated conditions) or muscle (experimental conditions). Coherence was calculated on 1 s long epochs of AI and compared to coherence values calculated from amplitude envelops (AE) of hdEMG and Cumulative Spike Trains (CST) calculated from individual MUs as identified by decomposition of hdEMG. Coherence values in AI (0.98±0.02 in synthetic and 0.49±0.20 in experimental conditions) were significantly higher than in the AE (0.89±0.07 in synthetic and 0.23 ± 0.15 in experimental conditions) and CST (0.83±0.11 in synthetic and 0.20 ± 0.10 in experimental conditions). The optimal extension factors were relatively high (>80), especially when compared to those for hdEMG decomposition (typically around 15). The reasons for this are not yet fully known and need further investigation.*

1 Introduction

In human movement science, functional coupling between the pools of motor units (MUs) has gained considerable attention in recent years, revealing common behaviour of MUs from different muscles and/or different behaviour of MUs from the same skeletal muscle (i.e. functional clusters of MUs) [5]. Different approaches to functional coupling assessment have been proposed. Still, coherence between the cumulative spike trains (CST) of MUs identified from high-density electromyograms (hdEMG) remains among the most accurate and frequently used ones [9][10]. However, its performance depends on the number of identified MUs [10], which is difficult to guarantee in all the experimental conditions.

Recently, we proposed using the activity index (AI) instead of CST [7][9] when estimating coherence. Similar to the CST, the AI compensates the shapes of Motor Unit Action Potentials (MUAPs) in the hdEMG but does not aim to identify the contributions of individual MUs. Instead, it directly estimates the smoothed (low-pass filtered) version of CST of all the MUs, which are active in the detection volume of the uptake hdEMG electrodes. The latter is usually considerably larger than the number of MUs identifiable from hdEMG [8]. The reason for this lies in the relatively small selectivity of hdEMG electrodes and, consequently, many small and/or deep MUs that contribute small MUAPs to the hdEMG. These MUs are not identifiable but rather contribute to the physiological noise. Also important, MUs that share the size, territory in the muscle tissue, location of the innervation zone and MUAP propagation velocity (i.e., conduction velocity), are very difficult to discriminate by hdEMG decomposition and get merged in the identified MU spike trains [8]. All these factors are hindering the number of individual MUs that can be identified by hdEMG decomposition.

As discussed in this contribution and in [9], MUAP compensation in AI and CST contributes to a more accurate coherence estimate. But MUAP compensation depends on the extension factor, i.e., the number of delayed repetitions of each hdEMG channel added in a preprocessing step. In this study, we investigated how much the extension factor influences the coherence estimation between pools of MUs.

2 Methods

2.1 Synthetic hdEMG

Synthetic hdEMG signals were generated by the cylindrical volume conductor model [1]. Two heads of Biceps Brachi (BB) muscle were simulated, each containing 200 MUs. 20 s of 9×10 sEMG channels were simulated and sampled at 2048 Hz. MU recruitments and discharges were generated using the model proposed in [2]. Constant excitation of 10%, 30% and 50% of maximum voluntary contraction (MVC) were simulated. 10 Hz sinusoidal modulation with an amplitude of 5% of MVC was superimposed. This resulted in the synchronisation of MU discharge patterns at 10 Hz.

2.2 Experimental hdEMG

Experimental hdEMG signals were acquired from gastrocnemius medialis (GM) and lateralis (GL) muscles during plantar flexion in 5 healthy young persons (age:

32±4 years). The study procedures were in accordance with the Declaration of Helsinki and were approved by the Medical Ethics Committee of the Republic of Slovenia (0120-84/2020/4). The procedures were explained to the participants, who gave written informed consent prior to their participation. 20 s long contractions at 10%, 30%, and 15 s long contractions at 50% and 70% of MVC were recorded by a hdEMG array of 13×5 electrodes (OT Bioelettronica, Torino, Italy), placed over each investigated muscle. The signals were amplified and sampled at 2048 Hz and 16-bit resolution (Quattrocento, OT Bioelettronica, Torino, Italy).

2.3 CKC Decomposition & Activity Index

In isometric non-fatiguing contractions, the hdEMG signals can be modelled as:

$$\boldsymbol{y}(n) = \mathbf{H}\mathbf{t}(n) + \boldsymbol{\omega}(n) \quad (1)$$

where $\boldsymbol{y}(n) = [y_1(n), y_1(n+1), \dots, y_1(n+F-1), y_2(n), \dots, y_M(n-F+1)]$ is vector of extended hdEMG channels at time sample *n*, *F* is extension factor, $\overline{\mathbf{H}} = \left[\overline{\mathbf{H_1}} \dots \overline{\mathbf{H_J}}\right]$ with

$$\overline{\mathbf{H_J}} = \begin{bmatrix} \overline{h_{1\mathrm{J}}}(0) & \dots & \overline{h_{1\mathrm{J}}}(L) \\ \vdots & \ddots & \vdots \\ \overline{h_{\mathrm{MJ}}}(0) & \dots & \overline{h_{\mathrm{MJ}}}(L) \end{bmatrix} \quad (2)$$

is a matrix of MUAPs, whereat $\overline{h_{\mathrm{IJ}}}(l)$ is the *l*-th sample of the MUAP from the j-th MU as detected in the *i*-th extended hdEMG channel. **L** is MUAP length in samples and **M** is the number of EMG channels. $\mathbf{t}(n)$ is a vector of spike trains from J MUs, active in the detection volume of uptake electrodes at time sample *n*:

$$t_{\mathrm{j}}(\mathrm{n}) = \sum_{\mathrm{k}} \delta\left(n - \tau_{\mathrm{j}}(k)\right) \quad (3)$$

with $\delta(.)$ denoting the unit response. $\boldsymbol{\omega}(n)$ is additive noise vector at sample *n*.

The Convolution Kernel Compensation (CKC) method [3] estimates the j-th MU spike train as:

$$\hat{t}_j(n) = \boldsymbol{c}_{t_j\boldsymbol{y}}^T \boldsymbol{C}_{\boldsymbol{y}}^{-1} \boldsymbol{y}(n) \approx \boldsymbol{c}_{t_j\boldsymbol{t}}^T \boldsymbol{C}_{\boldsymbol{t}}^{-1} \boldsymbol{t}(n) \quad (4)$$

where $\boldsymbol{C_y}$ and $\boldsymbol{C_{\bar{t}}}$ denote the correlation matrix of extended hdEMG channels and MU spike trains, respectively, and $\boldsymbol{c}_{t_j\boldsymbol{y}}^T$ denotes the blindly estimated vector of cross-correlations between the *j*-th MU spike train $t_j(n)$ and all hdEMG channels [3]. For clarity, the contribution of noise has been discarded. MU spike trains are then manually inspected, assessed for the accuracy of MU identification [4] and edited by experts. The resulting MU spike trains are summed up to form CST [11].

The MU activity index (AI) is defined as [3][7]:

$$AI(n) = \boldsymbol{y}(n)^T \boldsymbol{C_y}^{-1} \boldsymbol{y}(n) \approx \bar{\boldsymbol{t}}(n)^T \boldsymbol{C_{\bar{t}}}^{-1} \bar{\boldsymbol{t}}(n) \quad (5)$$

The AI compensates the MUAPs in **H** and reveals the CST of all the MUs in the detection volume. However, the compensation of **H** in Eq. (5) depends on the extension factor F and many other factors, including the anatomic properties of the investigated muscle and the electrical properties of uptake electrodes. In this study, we tested extension factors F between 1 and 5 (in increments of 1) and between 10 and 100 (in increments of 5).

In addition to AI and CST, we calculated the amplitude envelopes (AE) as an average rectified hdEMG value across all the hdEMG channels per muscle.

2.4 Coherence and Statistical Analysis

We calculated the AI, AE and CST for each investigated muscle (BB head in synthetic conditions) separately. Afterwards, we calculated the coherence between AIs, AEs and CSTs, revealing the functional coupling between the MU pools in these investigated muscles. In this study, we calculated the coherence across non-overlapping 1 s long epochs of activity indices.

Statistical analysis was conducted in Matlab, using the linear mixed effects (LME) models and taking the contraction level, extension factor F and hdEMG processing method (CST, AI or AE) as fixed factors and subjects (simulated muscles) as a random factor.

3 Results

3.1 Synthetic hdEMG

On average, 19±6 MUs were identified from each simulated BB head. Correlation among the identified AIs (one from each BB head) significantly depended on the extension factor F, and coherence increased up to extension factor F=80 (Figure 1). At an extension factor of F=80, AI exhibited significantly higher coherence value (0.978±0.016) than AE (0.886±0.072, $p<0.0001$) and CST (0.832±0.114, $p<0.0001$) (Figure 2 [6]). In AI, the coherence value of 0.89 was exceeded already at the extension factor of F = 1, demonstrating the superiority of AI over the AE.

3.2 Experimental hdEMG

On average, 12±8 and 4±3 MUs were identified from GM and GL, respectively. Noteworthy, the number of MUs identified from GL muscle was relatively low. This likely resulted in a decreased ability to estimate coherence from CST. Coherence between AIs increased significantly up to the extension factor F=100 (Figure 2). As depicted in Figure 4 [6], at an extension factor of F=100, AI (0.49 ± 0.20) exhibited significantly higher coherence values than AE (0.23 ± 0.15, $p<0.001$) and CST (0.20 ± 0.10, $p<0.001$). In AI, the average coherence value of 0.23 (average coherence value of AE) was exceeded at the extension factor of F = 15.

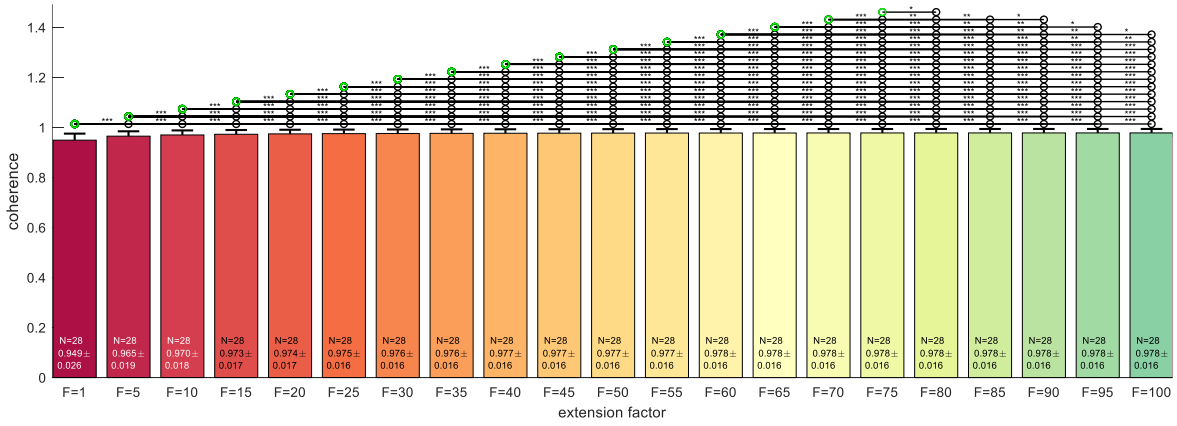

Figure 1. Impact of the extension factor F on the coherence between AIs from both BB heads (synthetic hdEMG); * - p<0.05, ** - p<0.01, *** - p<0.001

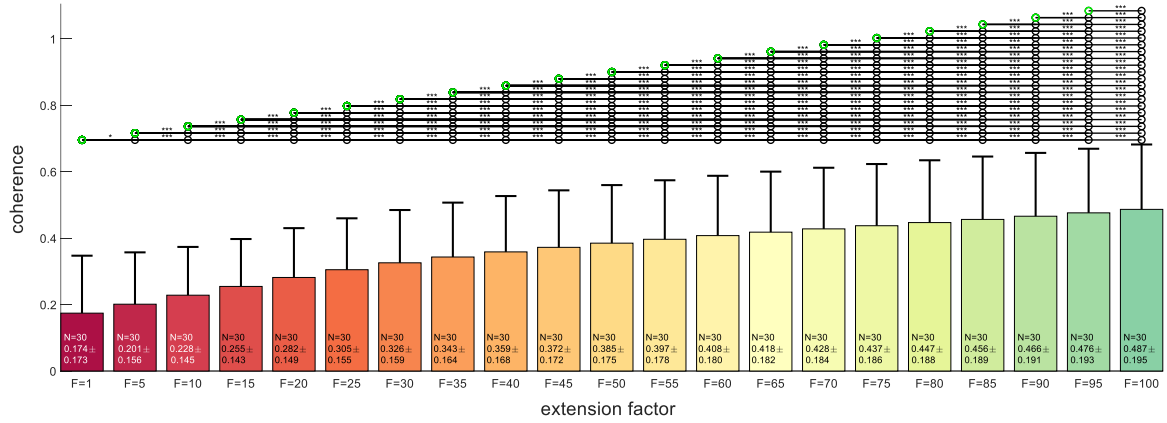

Figure 3. Impact of the extension factor F on the coherence between AIs from GM and GL muscle (experimental hdEMG); * - p<0.05, ** - p<0.01, *** - p<0.001

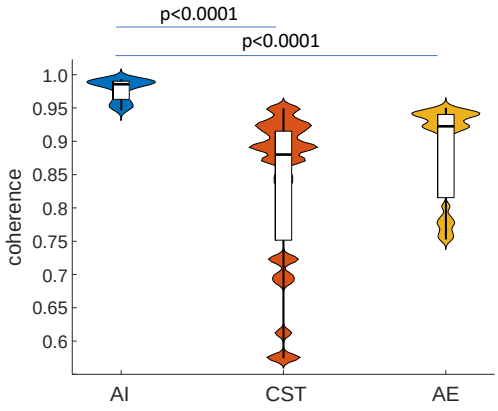

Figure 2. Violin plots comparing coherence estimation between the two heads of BB (synthetic hdEMG). AI was calculated using an extension factor of F = 80.

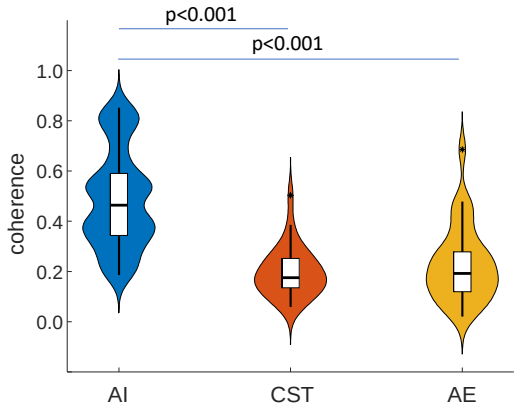

Figure 4. Violin plots comparing coherence estimation between GM and GL using AI, CST, and AE methods. AI was calculated using an extension factor of F = 100.

4 Discussion

We compared techniques for estimating muscle activity from hdEMG, namely, amplitude envelops (AE), CSTs as calculated from individual MUs identified by hdEMG decomposition and activity index (AI). CST and AI compensate for MUAP shapes and, therefore, expose the properties of MU spike trains and discharge patterns. On the other hand, the AE mixes spectral properties of MUAPs and MU spike trains. As MUAPs depend on the anatomical properties of investigated skeletal muscle, on the muscle geometry and the properties of uptake hdEMG electrodes, they hinder the information from the central nervous system that is reflected in the MU spike trains.

Compensation of MUAP shapes in CST and AI is rarely perfect. Indeed, hdEMG contains many more MUs active in the detection volume of uptake electrodes than the number of hdEMG channels. Consequently, the mixing matrix **H** has many more columns than rows and cannot be fully compensated in Eqs. (4) and (5). The level of its compensation depends on the extension factor F. For MU identification from hdEMG, the impact of extension factor F has been well investigated, demonstrating the optimal values of F in the range from 10 to 20 [3][4][10]. For AI, the impact of the extension factor is less clear and needs further investigation. Namely, AI contains the contributions of many more active MUs than CST.

In this study, we calculated the coherence between two heads of BB muscle (synthetic hdEMG) and GM and GL muscle (experimental hdEMG). We demonstrated that for AI, the optimal values of the extension factor extend well above the ones recommended for hdEMG decomposition. In synthetic cases, the coherence plateau was reached at extension factor F=80. In experimental conditions, it extended even further, all the way to F=100. The reasons for such a high F value are not fully understood and need further investigation. Although the coherence would likely increase in experimental conditions with F>100, we limited our investigation to the maximal value of F=100. The reason for this lies in the computational complexity of AI calculation. The latter grows quadratically with F. Indeed, on a personal computer with the Intel CORE i9 (9^{th} Gen) processor and 32 GB of memory, the AI calculation at F=1 and F=100 required 0.43 ± 0.08 s and 82.8 ± 4.3 s, respectively. Note that the longest processing times of AI still represent relatively small processing costs compared to MU identification from hdEMG, which typically requires 10 minutes.

AI significantly outperformed both AE and CST methodologies, already at much smaller than the optimal values of the extension factor F. The reasons for the inferior performance of AE likely originate from the lack of compensation for MUAPs, as already discussed. The performance of CST depends on the number of identified MUs. The latter was relatively low in our study, especially for GL muscle. Indeed, the number of identified MUs is frequently low, especially in proximal skeletal muscles or anatomically complex muscles, such as erector spinae or pectoralis muscle. In these muscles, the large number of active MUs and intensive low-pass filtering of adipose tissue hinder the identification of individual MUs [8]. Therefore, alternative methods that compensate for the negative effect of MUAPs but do not depend on individual MU identification are required. One of the possible approaches presented in this study is AI.

Acknowledgements

This research was funded by the European Union's Horizon Europe Research and Innovation Program [HybridNeuro project, GA No. 101079392] and by the Slovenian Research and Innovation Agency (Project J2-1731 and Programme funding P2-0041). Views and opinions expressed are, however, those of the author(s) only and do not necessarily reflect those of the European Union or Research Executive Agency. Neither the European Union nor the granting authority can be held responsible for them.

Bibliography

[1] Farina, D., Mesin, L., Martina, S. and Merletti, R. (2004), A surface EMG generation model with multilayer cylindrical description of the volume conductor. IEEE Transactions on Biomedical Engineering, 51(3), pp.415-426.

[2] Fuglevand, A.J., Winter, D.A. and Patla, A.E. (1993), Models of recruitment and rate coding organization in motor-unit pools. Journal of neurophysiology, 70(6), pp.2470-2488.

[3] Holobar A., Zazula D. (2007), Multichannel blind source separation using convolution kernel compensation, IEEE Transactions on Signal Processing, Vol. 55, pp. 4487-4496.

[4] Holobar A., Minetto M.A., Farina D. (2014), Accurate identification of motor unit discharge patterns from high-density surface EMG and validation with a novel signal-based performance metric. J Neural Eng 11, 016008.

[5] Hug, F., Avrillon, S., Sarcher, A., Del Vecchio, A. and Farina, D. (2023), Correlation networks of spinal motor neurons that innervate lower limb muscles during a multi-joint isometric task. The Journal of physiology, 601(15), pp.3201-3219.

[6] Karvelis P., (2024), Daviolinplot - beautiful violin and raincloud plots (https://github.com/povilaskarvelis/DataViz/releases/tag/v3.2.4), GitHub. Retrieved May 10, 2024.

[7] Kranjec, J. and Holobar, A., 2019. Improved assessment of muscle excitation from surface electromyograms in isometric muscle contractions. IEEE Transactions on Neural Systems and Rehabilitation Engineering, 27(7), pp.1483-1491.

[8] Kutoš, L., Škarabot, J. and Holobar, A. (2023). Identifikacija gruč neločljivih motoričnih enot iz večkanalnih površinskih elektromiogramov dvoglave nadlahtne mišice. ERK 2023 Conference.

[9] Kutoš L., Divjak M., Holobar A. (2024): Activity index outperforms cumulative spike train and amplitude envelopes in surface EMG coherence analysis, ISEK XXV Congress, Nagoya, Japan, June 26 – 29, 2024

[10] Muceli, S., Poppendieck, W., Holobar, A., Gandevia, S., Liebetanz, D. and Farina, D. (2022), Blind identification of the spinal cord output in humans with high-density electrode arrays implanted in muscles. Science advances, 8(46), p.eabo5040.

[11] Negro, F. and Farina, D., 2011. Decorrelation of cortical inputs and motoneuron output. Journal of Neurophysiology, 106(5), pp.2688-2697.